Myocilin Regulates Metalloprotease 2 Activity Through Interaction With TIMP3

Myung Kuk Joe,[1] Raquel L. Lieberman,[2] Naoki Nakaya,[1] and Stanislav I. Tomarev[1]

[1]Section of Retinal Ganglion Cell Biology, Laboratory of Retinal Cell and Molecular Biology, National Eye Institute, National Institutes of Health, Bethesda, Maryland, United States
[2]School of Chemistry and Biochemistry, Georgia Institute of Technology, Atlanta, Georgia, United States

Correspondence: Stanislav I. Tomarev, National Eye Institute, 6 Center Drive, Building 6, Room 212, Bethesda, MD 20892, USA; tomarevs@nei.nih.gov.

Submitted: July 15, 2016
Accepted: September 13, 2017

Citation: Joe MK, Lieberman RL, Nakaya N, Tomarev SI. Myocilin regulates metalloprotease 2 activity through interaction with TIMP3. *Invest Ophthalmol Vis Sci*. 2017;58:5308–5318. DOI:10.1167/iovs.16-20336

Purpose. To elucidate functions of wild-type myocilin, a secreted glycoprotein associated with glaucoma.

Methods. Lysates of mouse eyes were used for immunoprecipitation with affinity-purified antibodies against mouse myocilin. Shotgun proteomic analysis was used for the identification of proteins interacting with myocilin. Colocalization of myocilin and tissue inhibitor of metalloproteinases 3 (TIMP3) in different eye structures was investigated by a multiplex fluorescent in situ hybridization and immunofluorescent labeling with subsequent confocal microscopy. Matrix metalloproteinase 2 (MMP2) activity assay was used to test effects of myocilin on TIMP3 inhibitory action.

Results. TIMP3 was identified by a shotgun proteomic analysis as a protein that was coimmunoprecipitated with myocilin from eye lysates of wild-type and transgenic mice expressing elevated levels of mouse myocilin but not from lysates of transgenic mice expressing mutated mouse myocilin. Interaction of myocilin and TIMP3 was confirmed by coimmunoprecipitation of myocilin and TIMP3 from HEK293 cells transiently transfected with cDNAs encoding these proteins. The olfactomedin domain of myocilin is essential for interaction with TIMP3. In the eye, the main sites of myocilin and TIMP3 colocalization are the trabecular meshwork, sclera, and choroid. Using purified proteins, it has been shown that myocilin markedly enhanced the inhibitory activity of TIMP3 toward MMP2.

Conclusions. Myocilin may serve as a modulator of TIMP3 activity via interactions with the myocilin olfactomedin domain. Our data imply that in the case of *MYOCILIN* null or some glaucoma-causing mutations, inhibitory activity of TIMP3 toward MMP2 might be reduced, mimicking deleterious mutations in the *TIMP3* gene.

Keywords: myocilin, matrix metalloproteinase 2, TIMP3, glaucoma, olfactomedin

The myocilin (*MYOC*) gene was the first identified gene bearing mutations leading to both juvenile- and adult-onset primary open-angle glaucoma (POAG).[1,2] More than 70 pathogenic sequence variants in the *MYOC* gene have been identified to date, and they may contribute to approximately 8% to 36% and 2% to 4% of juvenile- and adult-onset POAG cases in different populations, respectively.[1,3–7] Most glaucoma-causing variants in the *MYOC* gene are located in the third exon encoding the olfactomedin (OLF) domain. Approximately 2.7 million people in the United States suffered from glaucoma in 2010, and this number is expected to increase to 4 million in 2030. Since POAG is the most common form of glaucoma, mutations in *MYOC* may contribute to more than 50,000 POAG cases, making mutations in this gene one of the most common causes of inherited eye disease with a known molecular basis.

The *MYOC* gene is expressed in several ocular and nonocular tissues with the highest levels of expression detected in the trabecular meshwork (TM) and sclera[1,2,8–10]; yet no pathologies besides glaucoma have been reported for patients carrying mutations in the *MYOC* gene. To study functions of myocilin in vivo, several mouse lines were developed carrying the *Myoc* null mutation, expressing mutated mouse and human myocilin, as well as expressing elevated levels of wild-type (WT) mouse myocilin.[11–16] *Myoc* null mice do not develop glaucoma but show defects in the myelination of the optic and sciatic nerve.[11,17,18] Transgenic (Tg) mice expressing elevated levels of WT mouse myocilin and mutated mouse and human myocilin have been produced using artificial bacterial chromosome DNA containing the full-length mouse or human *Myoc* gene and their long flanking sequences.[12–14] Tg mice producing approximately 15-fold higher levels of myocilin in the eye drainage structures and skeletal muscles than WT mice do not develop glaucoma but have increased skeletal muscle mass in the legs.[12,19] Aged (15–18 months old) Tg mice producing physiological levels of mutated human (Y437H) or mouse (Y423H) myocilin demonstrated a very moderate intraocular pressure (IOP) elevation and approximately 20% loss of retinal ganglion cells in the peripheral retina,[13,14] while mice with the Y423H knocking-in mutation did not show any glaucomatous changes.[15] Expression of the human Y437H mutant myocilin at a much higher level in the TM of Tg mice using the cytomegalovirus (CMV) promoter led to a more dramatic elevation of IOP and retinal ganglion cell (RGC) loss that could be detected even in 3- to 5-month-old mice.[16] Available data suggest that glaucoma-causing mutations in the *MYOC* gene lead to the production of protein that is not properly secreted

but retained in the endoplasmic reticulum (ER).[20–22] Accumulation of mutated myocilin in the ER of the TM induces ER stress with subsequent deterioration of TM functions.[16,23–26] Expression of mutated myocilin also makes TM cells more sensitive to oxidative stress.[27] In spite of all this information about myocilin in a glaucoma context, functions of WT myocilin are still poorly understood.

Identification of proteins interacting with myocilin is one of the possible approaches to elucidate its functions since interacting proteins are often involved in the same physiological processes and pathologies.[28–30] In this work, we identified tissue inhibitor of metalloproteinases 3 (TIMP3) as a protein interacting with myocilin. Our data demonstrate that the C-terminal OLF domain of myocilin is essential for its interaction with TIMP3. Moreover, myocilin may modulate TIMP3 activity toward matrix metalloproteinase 2 (MMP2). MMP2 is one of the most abundant MMPs in the TM, while sequence variants in the *TIMP3* gene are associated with a number of ocular and nonocular disorders.[31–33] Our findings justify further studies to test whether the absence of myocilin as well as some myocilin mutants may contribute to glaucoma and some other eye pathologies through an alteration of balance between MMP2 and TIMP3.

Methods

Animals

All experiments were performed with 2- to 4-month-old mice. Mice were maintained in accordance with guidelines described in the ARVO Statement for the Use of Animals in Ophthalmic and Vision Research, using protocols approved by the National Eye Institute Committee on the Use and Care of Animals. *Myoc* null mice, Tg expressing elevated levels of WT mouse myocilin, and Tg expressing Y423H mutated mouse myocilin have been described previously.[11–13] The FVRD nonpigmented mouse line was derived from the FVB/N line by replacing mutated *Pde6b* with the normal *Pde6b* allele. The normal *Pde6b* allele was backcrossed onto FVB/N for approximately 35 generations. FVRD mice have normal retinas without any detectable defects.

Antibodies and Plasmids

Anti-TIMP3 antibodies for immunofluorescent immunohistochemistry were purchased from Novus Biologicals (Littleton, CO, USA). Anti-FLAG and anti-myc antibodies were from Sigma-Aldrich Corp. (St. Louis, MO, USA); anti-HA-tag antibody was from Cell Signaling Technology (Danvers, MA, USA). Polyclonal rabbit antiserum against mouse myocilin was described previously.[11] Purified anti-myocilin antibodies were purified from anti-myocilin rabbit serum through an antigen-specific affinity purification. Normal rabbit IgG was purchased from Sigma-Aldrich Corp. Affinity-purified anti-myocilin antibodies were labeled with horseradish peroxidase (HRP) using the HRP conjugation kit (Abcam, Cambridge, MA, USA) according to the manufacturer's instructions. Human myocilin, myocilin-ΔC, and myocilin-ΔN constructs tagged with the FLAG epitope were previously described.[34] Mouse *Timp3* cDNA was cloned into the pcDNA3.1/Myc-His vector (Invitrogen, Carlsbad, CA, USA). Human full-length *TIMP2*, *TIMP3*, and *TIMP4* cDNAs were cloned into the pcDNA3 vector in-frame with hemagglutinin tag (HA).

Shotgun Proteomics

Mouse eyes were dissected; lens, cornea, and retina were removed; and the rest of the eyes were homogenized in IP buffer (25 mM Tris–HCl, pH 7.4, 1 mM EDTA, 150 mM NaCl, 1% NP-40, and 5% glycerol) containing a protease inhibitor mixture (Roche, Mannheim, Germany). Affinity-purified anti-myocilin antibody (10 μg) was cross-linked to protein A/G agarose beads using a crosslink IP kit (Thermo Fisher Scientific, Waltham, MA, USA). Following centrifugation, eye lysates were incubated with anti-myocilin beads or control rabbit IgG beads at 4°C overnight. The beads were washed five times with a lysis buffer, and proteins bound to the beads were eluted with an elution buffer (60 μL) provided with the IP kit. Samples from three different animals in each group were combined and used for further analysis.

Liquid chromatography-tandem mass spectrometry (LC-MC/MC) analysis was conducted as previously described[35] by Bioproximity, LLC (Chantilly, VA, USA). Briefly, eluted proteins were incubated in a solution of 2% SDS, 50 mM Tris–HCl (pH 7.6), and 10 mM dithiothreitol (DTT) at 95°C for 10 minutes. Samples were then transferred to a 30 K Amicon MWCO device (EMD Millipore, Billerica, MA, USA) and centrifuged at 13,000*g* for 30 minutes. The remaining samples were buffer exchanged with 6 M urea, 100 mM Tris–HCl, pH 7.6, then alkylated with 55 mM iodoacetamide. Trypsin was added at a 1:40 enzyme to substrate ratio and the samples were incubated overnight on a heat block at 37°C. Digested peptides were desalted using C18 stop-and-go extraction (STAGE) tips and then fractionated by strong anion exchange STAGE tip chromatography. Peptides eluted from the C18 STAGE tip were dried, and each reaction mixture was analyzed by LC–MS/MS. LC was performed on an Easy nanoLC II HPLC system (Thermo Fisher Scientific). The LC was interfaced to a dual pressure linear ion trap mass spectrometer (LTQ Velos; Thermo Fisher) via nano-electrospray ionization. The mass spectrometer was programmed to acquire, by data-dependent acquisition, tandem mass spectra from the top 15 ions in the full scan from 400 to 1400 m/z. Dynamic exclusion was set to 30 seconds. Mass spectrometer RAW data files were converted to MGF format using msconvert (http://proteowizard.sourceforge.net, in the public domain). Detailed search parameters are printed in the search output XML files. All searches required strict tryptic cleavage, 0 or 1 missed cleavage, fixed modification of cysteine alkylation, variable modification of methionine oxidation, and expectation value scores of 0.01 or lower. MGF files were searched using X!Hunter[36] against the latest library available on the Global Proteome Machine Database (GPMDB) at the time. Other searches used the cRAP contaminant library from the GPMDB and libraries constructed from the latest Ensembl release available at the time. MGF files were searched using X!!Tandem[37] using both the native and the k-score scoring. All searches were performed on Amazon Web Services–based cluster compute instances using the Proteome Cluster interface (https://www.proteomecluster.com, in the public domain). XML output files were parsed and nonredundant protein sets determined using MassSieve (https://www.ncbi.nlm.nih.gov/staff/slottad/MassSieve, in the public domain). Proteins were required to have two or more unique peptides across the analyzed samples with *E* value scores of 0.01 or less, 0.001 for X!Hunter, and protein *E* value scores of 0.0001 or less.

Transfection, Immunoprecipitation, and Western Blotting

HepG2 and HEK293 cells were transiently transfected with indicated DNA constructs using Lipofectamine 2000 (Thermo Fisher Scientific) and seeded in six-well culture dishes. Cells were washed with PBS and lysed in IP buffer containing a protease inhibitor mixture (Roche) as described above. After

Investigative Ophthalmology & Visual Science

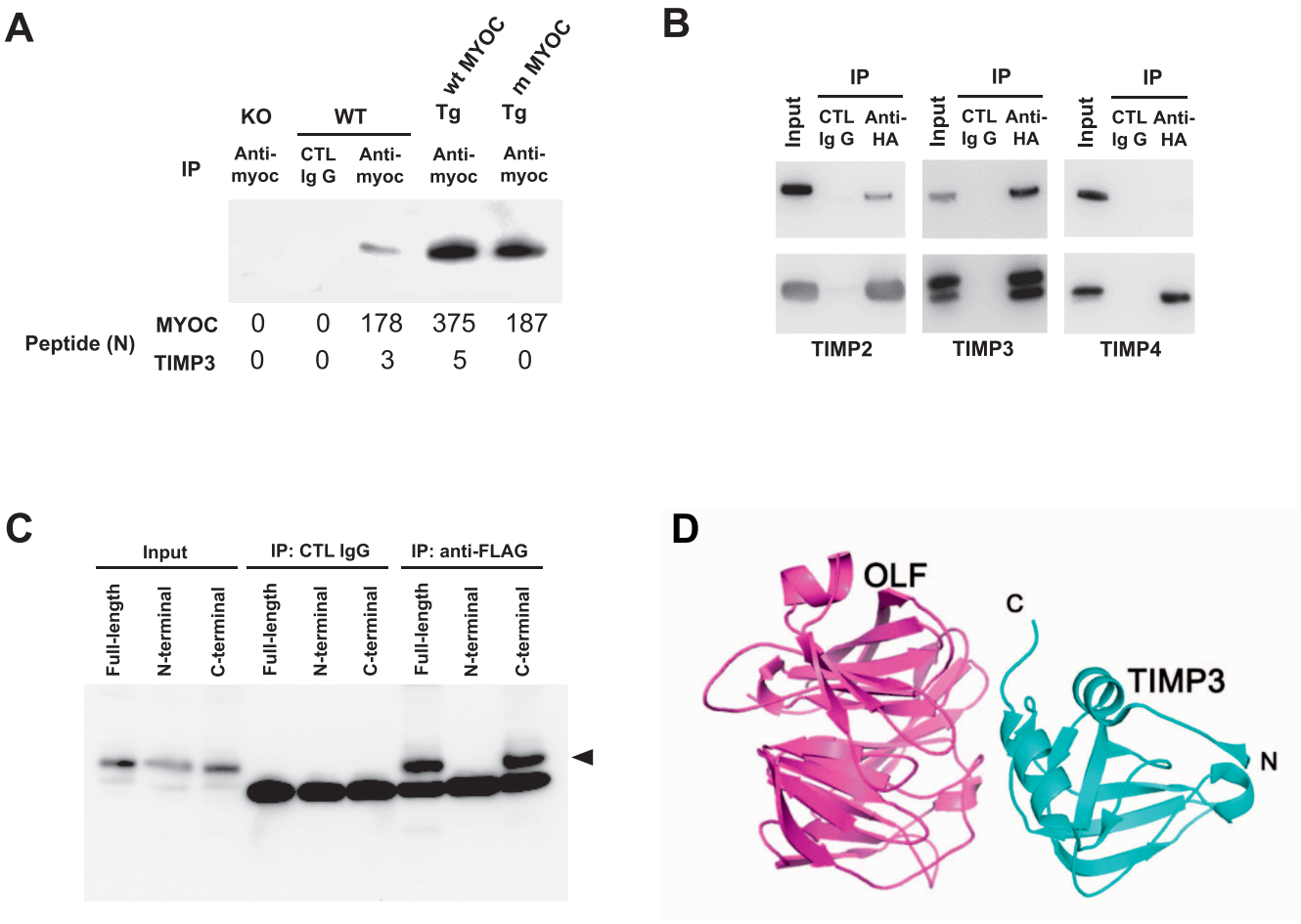

Figure 1. TIMP3 is identified as a myocilin-binding protein. (**A**) Western blot analysis of immunoprecipitates with anti-myocilin antibodies or rabbit IgG from eye lysates of *Myoc* null (KO), WT, and Tg mice expressing WT (wt MYOC) or mutated mouse myocilin (m MYOC). The efficiency and specificity of immunoprecipitation were confirmed using anti-myocilin antibodies. The peptide number (*N*) indicates the number of peptides associated with myocilin (MYOC) or TIMP3 identified in the immunoprecipitates by shotgun proteomics. (**B**) Myocilin interacts with TIMP3 in HEK293 cells. HEK293 cells were cotransfected with indicated HA-tagged human TIMP constructs and a FLAG-tagged human myocilin construct. The lysates were immunoprecipitated with anti-HA antibodies and the precipitates were probed with anti-FLAG antibodies. (**C**) Myocilin interacts with TIMP3 in HepG2 cells. HepG2 cells were cotransfected with a myc-tagged TIMP3 construct and indicated FLAG-tagged myocilin constructs. The lysates were immunoprecipitated with anti-FLAG antibodies and the precipitates were probed with anti-myc antibodies. The *arrowhead* marks TIMP3 band and the *arrow* marks immunoglobulin band. (**D**) Model of TIMP3–OLF interaction based on computational docking, suggesting that OLF does not compete for the MMP binding site on TIMP3, which is near its N-terminus.

centrifugation, soluble lysates were incubated with control rabbit IgG, anti-HA, or anti-FLAG antibodies for 2 hours at 4°C followed by incubation with 30 µL protein G-agarose beads (Roche) overnight at 4°C. The bead–antibody complexes were collected by centrifugation, rinsed three times in the IP buffer, resuspended in 1× Laemmli sample buffer, boiled for 5 minutes, separated by 4% to 12% gradient NU-PAGE (Invitrogen), and transferred to a nitrocellulose membrane (Invitrogen). Membranes were preincubated in a blocking buffer (5% nonfat milk, 25 mM Tris, 150 mM NaCl, 0.05% Tween 20, pH 7.4) and then incubated in a blocking buffer overnight at 4°C with corresponding primary antibodies. Secondary antibodies (an anti-rabbit or anti-mouse horseradish peroxidase antibodies; GE Healthcare Life Sciences, Issaquah, WA, USA) were diluted 1:5000 in a blocking buffer and incubated for 2 hours at room temperature. The immunoreactive bands were developed using SuperSignal WestDura (Thermo Fisher Scientific).

Computational Modeling of the Interaction Between the Myocilin Olfactomedin Domain and TIMP3

Coordinates of TIMP3 (PDB code 3CKI, Chain B corresponding to residues) as receptor and those of WT myocilin OLF domain (PDB code 4WXQ) as ligand were submitted to the ClusPro protein docking server. Coordinates of TIMP3 (PDB code 3CKI, Chain B corresponding to residues 1-121) as receptor and those of WT myocilin OLF domain (PDB code 4WXQ) as ligand were submitted to the ClusPro protein docking server.[38] The top 10 docked models were interrogated manually by comparing cluster score output from ClusPro and visually inspecting binding mode in Coot.[39] Based on these considerations, the presented docking model was evaluated as a plausible representation of the biological system. Figures were generated using PyMOL (www.pymol.org; in the public domain).

Investigative Ophthalmology & Visual Science

Single-Copy mRNA Detection by a Multiplex Fluorescent In Situ Hybridization

Tissue distribution of *Myoc* and *Timp3* mRNAs was investigated using RNAScope, a multiplex fluorescent in situ hybridization (fISH) following the manufacturer's instructions (Advanced Cell Diagnostics, ACD Bio; Newark, CA, USA). Mouse *Myoc* and *Timp3* hybridization probes were designed and provided by the manufacturer. Briefly, 2-month-old C57BL/6J males were euthanized and dissected eyes were fresh frozen in liquid nitrogen within 3 minutes after dissection. Frozen eyes were embedded in the optimal cutting temperature compound and 14-µm cryosections were prepared. Sections were fixed with 4% paraformaldehyde (PFA) for 15 minutes on ice, dehydrated by graded alcohol, and then dried. The specimens were pretreated with protease VI solution for 30 minutes at room temperature and then washed twice with PBS. The RNAScope (version 2.5, multiplex) fISH was performed using HybEZ oven (ACD Bio) according to the manufacturer's instructions. fISH results were analyzed using Zeiss LSM 700 confocal microscope (Carl Zeiss, Jena, Germany) and ZEN software.

Confocal Fluorescent Immunohistochemistry

Two-month-old FVRD or C57BL/6J mice were euthanized; eyes were dissected and fresh frozen in liquid nitrogen within 3 minutes after dissection. Frozen eyes were embedded in the optimal cutting temperature compound and 20-µm cryosections were prepared. Sections were fixed with 4% PFA for 10 minutes on ice, blocked with Blocker Casein PBS (Thermo Fisher) for 30 minutes at room temperature, and then incubated with primary antibodies against mouse myocilin or TIMP3 (Novus Biologicals) at 4°C overnight. After routine wash with PBS-0.05% Tween 20 (PBS-T), the sections were incubated with Alexa-555–labeled anti-rabbit IgG secondary antibodies and Hoechst 33342 at room temperature for 1 hour. Specimens were washed with PBS-T and mounted in FluorSave (Calbiochem, San Diego, CA, USA). The stained sections were analyzed using Zeiss LSM 700 confocal microscope and ZEN software.

Protein Purification

FLAG-tagged recombinant myocilin was expressed from a previously established HEK293 stable cell line.[23] Most of expressed myocilin was secreted and collected in serum-free conditioned medium. IP buffer was added to the myocilin containing conditioned medium. After centrifugation, the soluble supernatant was incubated with pre-equilibrated anti-FLAG M2 agarose beads (Sigma-Aldrich Corp.) at 4°C overnight with gentle rotation. After incubation, beads were collected and washed four times with IP buffer. Myocilin was eluted with the FLAG peptide (Sigma-Aldrich Corp.) in IP buffer. The purity of myocilin was assessed using SDS-PAGE.

MMP Activity Assay

Recombinant TIMP3 (50–400 nM) expressed and purified from NSO cells (Sigma-Aldrich Corp.) was incubated with MMP2 proenzyme (50 nM; EMD Millipore) for 2 hours. MMP2 was then activated by the addition of 1 mM p-aminophenyl mercuric acetate (Sigma-Aldrich Corp.) at 37°C for 1 hour and activity of MMP2 measured using EnzChek Gelatinase/Collagenase assay kit (Invitrogen) containing dye-quenched gelatin as a substrate, according to the manufacturer's instructions. To evaluate the effect of myocilin on TIMP3 inhibition of MMP2, 100 nM TIMP3 was preincubated for 2 hours with purified myocilin (200 nM) prior to adding the mixture to MMP2 for assay as above. *P* values were determined by a 2-tailed Student's *t*-test.

Results

Identification of TIMP3 as a Novel Myocilin-Binding Protein

To identify proteins interacting with myocilin in the eye tissues, we performed shotgun proteomic analysis of proteins that coimmunoprecipitated with myocilin in the eye lysates. We have used polyclonal affinity-purified antibodies against mouse myocilin that in our previous experiments efficiently precipitated myocilin-binding partners from ocular and non-ocular tissues.[19] Lens and neural retina were removed from dissected eyes before preparation of lysates because they are protein-rich anatomic structures that do not contain myocilin.[9,40,41] Lysates were prepared from WT Tg mice expressing elevated levels of WT mouse myocilin, Tg mice expressing mutated mouse myocilin (Y423H), as well as from *Myoc* null mouse eye lysates as a negative control. As an additional negative control, WT mouse eye lysates were immunoprecipitated with normal rabbit IgG. The eluted immunoprecipitates were analyzed by Western blotting with antibodies against mouse myocilin to confirm efficiency of immunoprecipitation. Eluted myocilin was detected in eluted immunoprecipitates from lysates of WT and Tg mice. As expected, a higher amount of myocilin was precipitated from Tg than from WT lysates (Fig. 1A). No myocilin was detected in eluted immunoprecipitates from *Myoc* null mice or in eluted immunoprecipitates obtained with control IgG (Fig. 1A). The eluted precipitated protein mixtures were analyzed by shotgun proteomic analysis. Eighty-three proteins were specifically identified in the myocilin antibody immunoprecipitates from WT and/or Tg samples. None of these proteins was identified in myocilin antibody immunoprecipitates from *Myoc* null or in control rabbit IgG immunoprecipitates from WT samples. The highest number of peptide spectral matches in immunoprecipitates from WT and Tg mice corresponded to myocilin, while no myocilin peptides were identified in negative controls (*Myoc* null mice and rabbit IgG, Fig. 1A). TIMP3 was one of the proteins copurified with myocilin. Three and five TIMP3 peptides were detected in the immunoprecipitates of WT and Tg mice expressing WT myocilin, respectively (Fig. 1A). No TIMP3 peptides were detected in the immunoprecipitates from negative control samples as well as in the immunoprecipitates from eyes of Tg mice expressing mutated mouse myocilin (Fig. 1A). We selected TIMP3 for more detailed analysis because it is a secreted protein involved in a number of ocular disorders.[31–33]

To confirm interaction between myocilin and TIMP3, we used several commercially available antibodies against TIMP3 for immunoprecipitation from the eye lysate of WT, Tg, and *Myoc* null mice with subsequent analysis of immunoprecipitates using myocilin antibodies and vice versa. The results of these experiments were not consistent. Because of that, we tested interaction of myocilin and TIMP3 in transiently transfected HEK293 cells. Two other TIMP proteins (TIMP2 and TIMP4) were also included in these experiments to test their ability to interact with myocilin and as additional controls. In transiently transfected cells, myocilin was more efficiently coimmunoprecipitated with TIMP3 than with TIMP2 and was not precipitated with TIMP4 (Fig. 1B). Based on these data, we concluded that myocilin may form a complex with TIMP3.

Investigative Ophthalmology & Visual Science

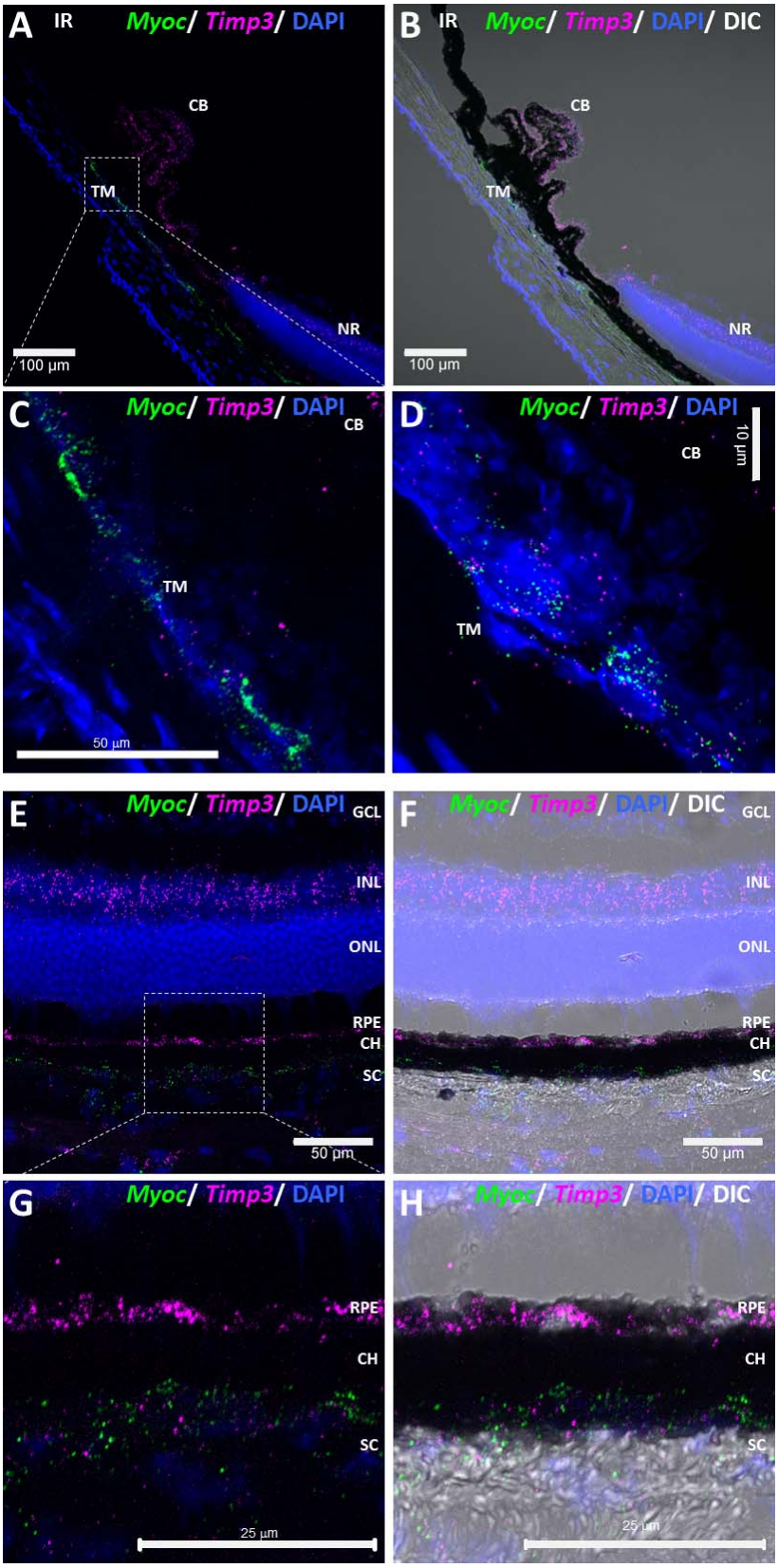

Figure 2. The distribution of *Myoc* and *Timp3* mRNAs in the eye drainage structures and in the posterior part of the eye. (**A–D**) Eye drainage structures: (**A**) *Myoc* mRNA (*green puncta*) is abundant in TM cells. *Timp3* mRNA (*magenta puncta*) is abundant in the ciliary body and is also present in TM cells. (**B**) The image of the same area shown in (**A**) obtained using differential interference contrast (DIC) microscopy for better visualization of the tissue orientation. It also reveals that *Timp3* mRNA is present in nonpigmented ciliary epithelium. (**C**) A magnified image of the TM area *boxed* in (**A**). (**D**) A further magnified image of the TM area. TM cells contain both *Myoc* and *Timp3* mRNAs. CB, ciliary body; IR, iris; NR, neural retina; SC, sclera; TM, trabecular meshwork. (**E–H**) Posterior part of the eye: (**E**) *Myoc* mRNA was detected in choroid in the proximity of

sclera and sclera. *Timp3* mRNA is abundant in the inner nuclear layer of the retina and RPE, and is also detected in choroid in the proximity of sclera. (**F**) The image of the same area as in (**E**) obtained using DIC microscopy. (**G**) A magnified image of the area *boxed* in (**E**). (**H**) The image of the same area as in (**G**) obtained using DIC microscopy to show the tissue orientation. CH, choroid; GCL, ganglion cell layer; INL, inner nuclear layer; ONL, outer nuclear layer; RPE, retinal pigmented epithelium; SC, sclera.

The C-Terminal OLF Domain of Myocilin Is Essential for the Interaction With TIMP3

To identify regions in myocilin responsible for the interaction with TIMP3, we performed coimmunoprecipitation experiments after cotransfection of HepG2 cells with myc-tagged TIMP3 and three different myocilin constructs, encoding full-length myocilin and its 22-kDa N-terminal (myocilin-ΔC) or 33-kDa C-terminal domains (myocilin-ΔN or OLF domain) fused to a FLAG tag. Since mouse and human TIMP3 proteins are 96% identical, we used available mouse TIMP3 expression construct in these experiments. TIMP3 was coprecipitated with full-length myocilin and its C-terminal domain, but not with the N-terminal myocilin domain (Fig. 1C). This indicates that the C-terminal myocilin domain is essential for interaction with TIMP3, a result supported by favorable energetics from computational docking of the myocilin OLF domain[42] onto the N-terminal TIMP3 inhibitory domain, on a site distinct from that of MMP binding[43] (Fig. 1D).

Coexpression of the *Myoc* and *Timp3* Genes in the Ocular Tissues

The distribution of both myocilin and TIMP3 in the eye structures has been investigated in multiple publications.[1,2,8–10,44,45] To localize more precisely the sites of *Myoc* and *Timp3* coexpression in the eye, we used high-resolution fISH, which enables quantification of mRNA expression levels simultaneously at the cellular resolution.

In the eye drainage structures, the *Myoc* gene, as expected, was preferentially detected in the TM area, while the *Timp3* mRNA was preferentially detected in the ciliary body with a lower level of expression in the TM area (Figs. 2A–D). In the posterior part of the eye, the *Myoc* mRNA was preferentially detected in the sclera as well as in the choroid at the proximity of sclera (Figs. 2E–H). The main sites of the *Timp3* gene expression were cells in the inner nuclear layer of the retina, retinal pigmented epithelium (RPE), and sclera. A few cells in the choroid at the interface with sclera also expressed *Timp3*. Thus, the main sites of *Myoc* and *Timp3* gene coexpression in the eye are the TM area, sclera, and outer layer of the choroid adjacent to the sclera.

Colocalization of Myocilin and TIMP3 in the Eye Tissues

Both myocilin and TIMP3 are secreted proteins. Therefore, the distribution of these proteins may differ from the distribution of their respective mRNAs. To examine colocalization of myocilin and TIMP3 proteins in ocular tissues, we conducted fluorescent immunohistochemistry. Immunostaining of C57BL/6J mouse eye sections with TIMP3 antibodies demonstrated that the Bruch's membrane showed much stronger immunofluorescence than RPE (not shown). Since melanin pigment is abundant in many ocular tissues (RPE, choroid, ciliary body) and has the potential to quench immunofluorescence in these tissues, we used unpigmented mouse strain FVRD in subsequent experiments. Because available antibodies against myocilin[11] and TIMP3[46] that work well with mouse tissues were both rabbit polyclonal antibodies, we independently stained adjacent sections with antibodies against myocilin or TIMP3. In the eye drainage structures, myocilin was detected in the TM (Figs. 3A–C), while TIMP3 was detected in the TM and ciliary body (Figs. 3G–I). In the posterior part of the eye, myocilin was detected in the sclera and in choroid (Figs. 3D–F). TIMP3 was detected in RPE, Bruch's membrane, choroid, and sclera (Figs. 3J–L). Thus, expanding on results from fISH, the main sites of myocilin and TIMP3 colocalization in the eye tissues at the protein level are the TM, choroid, and sclera.

Effect of Myocilin on TIMP3 Activity

To test the effect of myocilin on the inhibitory activity of TIMP3, we employed an MMP2 fluorescence activity assay. MMP2 was selected because it is expressed in both TM and sclera, is the most abundant MMP in the TM and anterior chamber,[47,48] and changes in the level of MMP2 activity can lead to eye pathologies including glaucoma, myopia, and age-related macular degeneration.[49–51] The purity of TIMP3 and myocilin used for the study was higher than 95% as assessed by SDS-PAGE (Fig. 4A).

To assess TIMP3 activity, we measured the gelatinase activity of MMP2 using a fluorescein conjugate–gelatin substrate. MMP2 hydrolyzes fluorescein-conjugated gelatin as seen by the increase in fluorescence over time upon incubation with different concentrations of MMP2 (Figs. 4B, 4C). Myocilin alone did not inhibit MMP2 activity (not shown). The proteolytic activity of MMP2 was efficiently inhibited by increasing concentrations of TIMP3 (Fig. 4B). We chose a TIMP3 concentration (100 nM) that produced a mild inhibition of MMP2 (50 nM) to evaluate the effect of myocilin on TIMP3 inhibition of MMP2. The proteolytic activity of MMP2 was more markedly inhibited when we added the TIMP3 together with myocilin versus TIMP3 alone, while addition of mouse IgG used as a negative control protein had no effect on TIMP3 activity (Fig. 4C).

Discussion

Taken together, by comparing results from shotgun proteomics in myocilin-relevant mouse models plus validation assays in transiently transfected cells and with purified proteins, we identified TIMP3 as a candidate interaction partner for the myocilin. OLF domain of myocilin is essential for interaction with TIMP3. It is interesting to note that Olfactomedin 1, another OLF domain–containing protein that we tested, did not bind TIMP3 when these two proteins are produced in transiently transfected cells (not shown). TIMP2 but not TIMP4 also appears to interact with myocilin (Fig. 1B), although we did not investigate this interaction in detail.

TIMP3 is a well-known inhibitor of MMPs and MMPs with thrombospondin motifs (ADAMTSs).[52] MMPs have multiple physiological functions including extracellular matrix remodeling, apoptosis, and cell migration and proliferation, among which the latter have also been linked to myocilin.[53–55] Mutations in the *TIMP3* gene may contribute to a number of ocular disorders including Sorsby's fundus dystrophy[31] and age-related macular degeneration (AMD).[32,33] Changes in MMP activity are associated with neurodegenerative disorders including glaucoma, AMD, and proliferative diabetic retinopathy.[56,57] Specific to glaucoma, changes in MMP2 (among other MMPs) activity may be involved in the regulation of IOP, which

Investigative Ophthalmology & Visual Science

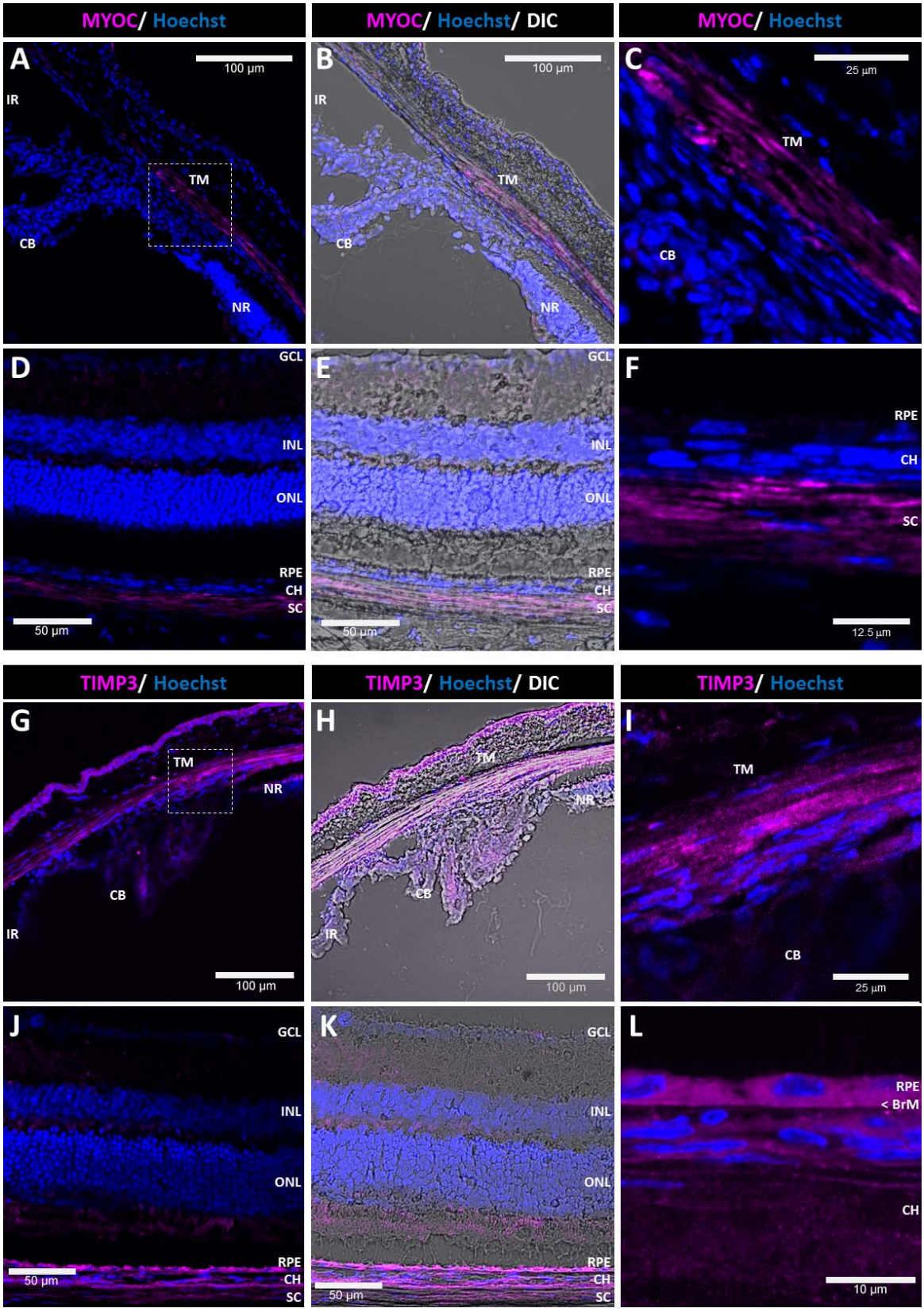

Figure 3. Distribution of myocilin and TIMP3 in the ocular tissues. Cryosections of the FVRD mouse eyes were stained with anti-myocilin and TIMP3 antibodies. (**A–C**, **G–I**) Eye drainage structures: (**A**) Myocilin is detected mainly in the TM. (**B**) The image of the same area as in (**A**) obtained using DIC microscopy for better visualization of the tissue orientation. (**C**) Enlarged image of the TM area *boxed* in (**A**). (**G**) TIMP3 is detected in the TM and ciliary body. (**H**) The image of the same area as in (**D**) obtained using DIC microscopy. (**H**) Enlarged image of the TM area *boxed* in (**G**). (**D–F**, **J–L**) Posterior part of the eye: (**D**) Myocilin was detected in the choroid and sclera. (**E**) The image of the same area as in (**D**) obtained using DIC microscopy. (**F**) Enlarged image of the RPE–sclera region. (**J**) TIMP3 was detected in the RPE, Bruch's membrane, choroid, and sclera. (**K**) The image of the same area as in (**J**) obtained using DIC microscopy. (**L**) An enlarged image of RPE–sclera region. Abbreviations are as in Figure 2. BrM, Bruch's membrane.

Investigative Ophthalmology & Visual Science

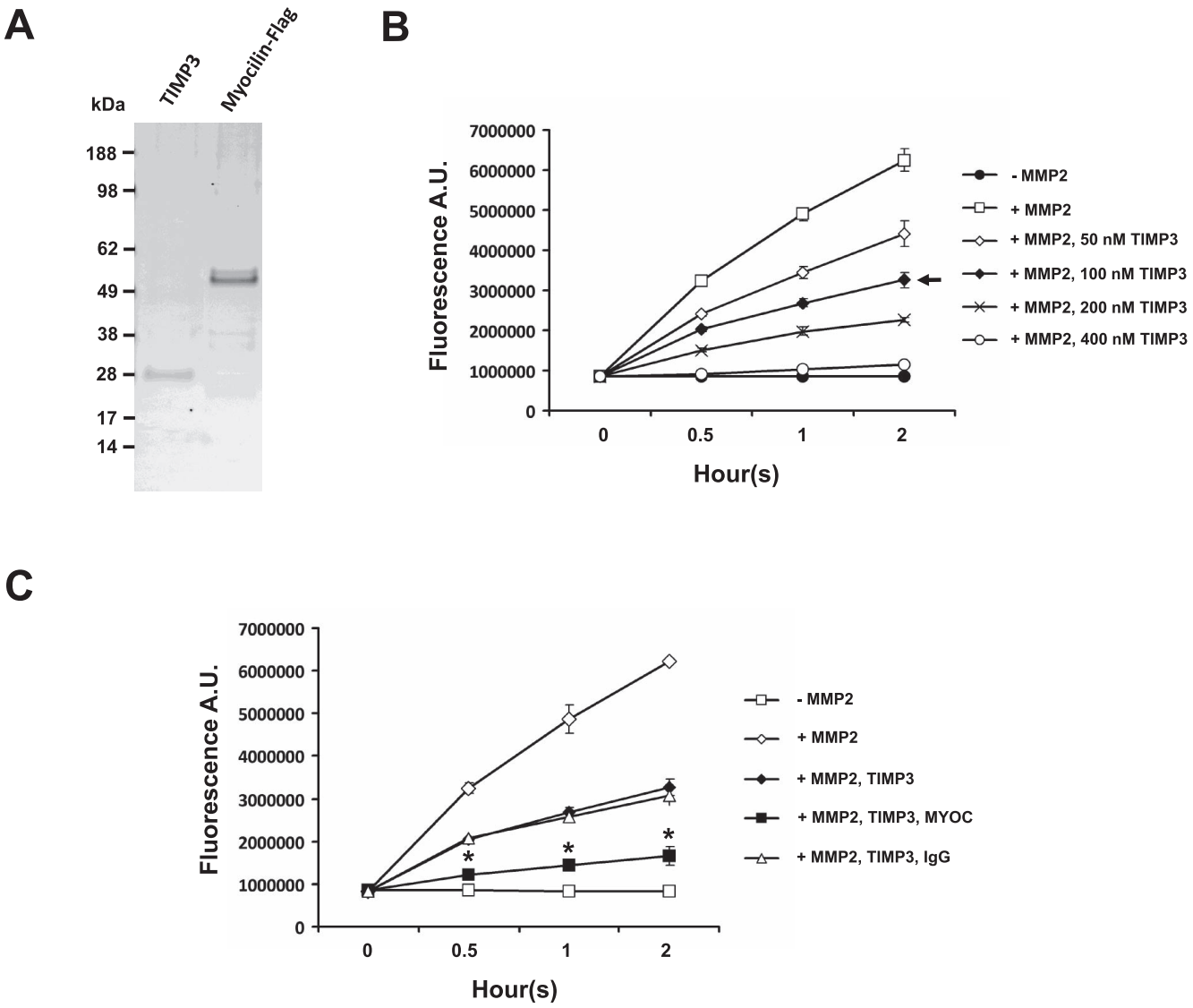

Figure 4. Myocilin enhances the inhibitory activity of TIMP3 toward MMP2. (**A**) The purity of TIMP3 and myocilin was estimated by SDS-PAGE. (**B**) MMP2 (50 nM) was coincubated with indicated different concentrations of TIMP3. The fluorescence signals representing the protease activity of MMP2 were monitored for 2 hours. *Arrow* indicates TIMP3 concentration selected for further studies. (**C**) Myocilin (200 nM) or control IgG (200 nM) was preincubated with TIMP3 (100 nM). TIMP3 alone or the protein mixtures were added to the MMP2 proteolytic reaction. *Error bars* represent ±SD of triplicate reactions. Statistically significant differences between two groups (+ MMP2, TIMP3 and + MMP2, TIMP3, MYOC) at different time points are indicated by *asterisks* ($P < 0.05$).

is thought to predominantly involve the TM tissue where both TIMP3 and myocilin were present in our study.[58,59] The upregulation of several MMP mRNAs including MMP2 mRNA has been reported in a steroid-induced mouse glaucoma model,[60] and MMP2 was also moderately increased in the TM and aqueous humor of patients with POAG as compared with healthy individuals.[48,61,62] Furthermore, changes in the balance between proteases and protease inhibitors (TIMP3) may modify choroid thickness.[63] A decrease in choroid thickness is associated with a number of eye disorders including myopia and AMD.[64–66]

Using purified TIMP3 and myocilin, we demonstrated that myocilin may increase inhibitory activity of TIMP3 toward MMP2 (Fig. 4). Myocilin effects on the activity of TIMP3 toward other MMPs or ADAMTSs, as well as the ability of myocilin to bind other members of TIMP family (TIMP1, TIMP2, and TIMP4), are worth studying in the near future.

TIMP3 is difficult to extract from tissues and it binds tightly to the extracellular matrix.[67] This property of TIMP3 suggests that TIMP3 should act in the vicinity of the sites of its synthesis. The tissue distribution of TIMP3 has been studied in mammalian tissues including ocular tissues. In the eye, TIMP3 was preferentially detected in RPE, Bruch's membrane, ciliary epithelium, and TM.[45,68–70] Our data on the distribution of *Timp3* mRNA and encoded protein (Figs. 2, 3) in general corresponded to the previously published results. In addition, using a high-resolution fISH, we demonstrated that *Timp3* mRNA is also abundant in the inner nuclear layer of the retina. Previous in situ hybridization experiments in which a digoxigenin-labeled *Timp3* riboprobe was used detected *Timp3* mRNA only in the RPE and to a minor extent in the ciliary epithelium of BALB/cJ mice.[71] These differences are explained by the significantly higher sensitivity of in situ hybridization method that we used in the current work. Indeed, *Timp3* mRNA has been recently detected in mouse

Investigative Ophthalmology & Visual Science

amacrine cells by drop-seq analysis.[72] It is interesting to note that TIMP3 protein is not detectable in the inner nuclear layer of the retina. This discrepancy between mRNA and protein data could be explained by a very efficient secretion of TIMP3 from cells in the inner nuclear layer or by nonefficient translation of *Timp3* mRNA in these cells. In unpigmented mouse eye, the level of TIMP3 immunostaining was high in both RPE and Bruch's membrane. Pigmented eyes demonstrated stronger TIMP3 immunofluorescence in the Bruch's membrane compared with RPE. We believe that quenching of immunofluorescence by melanin pigment may explain these differences. In the human eye, TIMP3 staining of the Bruch's membrane is normally stronger than in the RPE.[73] In addition, TIMP3 labeling in Bruch's membrane in human donor eyes has been reported to increase with age.[70] In contrast, mice used in this study were juveniles (2 months old).

The expression of the *Myoc* gene and encoded protein was detected in the expected eye structures: the TM and sclera. It was stated in several publications that the *Myoc* gene is also expressed in the RPE/choroid.[9,41] A high-resolution fISH allowed us to demonstrate that choroid cells located in the proximity of sclera but not RPE are the main site of *Myoc* expression (Fig. 2). Expression patterns of myocilin and TIMP3 demonstrate that the principal sites of their interactions are the TM area and interface of choroid and sclera.

In conclusion, these data suggest that myocilin is involved in the modulation of MMP2 activity via interaction with TIMP3 in the TM, choroid, and sclera. In the case of *MYOC* null or some glaucoma-causing mutations, inhibitory activity of TIMP3 toward MMP2 (and probably some other MMPs) might be compromised in the eye. If mutations in the *TIMP3* and *MYOC* genes are present together, this may lead to more severe eye pathologies compared with cases where only one of these genes is mutated.

Acknowledgments

The authors thank Yuriko Minegishi, PhD, for her help with in situ hybridization and immunostaining, Luis Bonet-Ponce, PhD, for his help with coimmunoprecipitation experiments, Robert Fariss, PhD, and Irina Karavanova, PhD, for their advice on immunostaining and in situ hybridization, respectively, and Ben Mead, PhD, for critical reading of the manuscript.

Supported by the Intramural Research Programs of the National Eye Institute, National Institutes of Health, and R01EY021205 to RLL.

Disclosure: **M.K. Joe**, None; **R.L. Lieberman**, None; **N. Nakaya**, None; **S.I. Tomarev**, None

References

1. Stone EM, Fingert JH, Alward WL, et al. Identification of a gene that causes primary open angle glaucoma. *Science*. 1997; 275:668–670.
2. Adam MF, Belmouden A, Binisti P, et al. Recurrent mutations in a single exon encoding the evolutionarily conserved olfactomedin-homology domain of TIGR in familial open-angle glaucoma. *Hum Mol Genet*. 1997;6:2091–2097.
3. Fingert JH, Heon E, Liebmann JM, et al. Analysis of myocilin mutations in 1703 glaucoma patients from five different populations. *Hum Mol Genet*. 1999;8:899–905.
4. Kwon YH, Fingert JH, Kuehn MH, Alward WL. Primary open-angle glaucoma. *N Engl J Med*. 2009;360:1113–1124.
5. Alward WL, Fingert JH, Coote MA, et al. Clinical features associated with mutations in the chromosome 1 open-angle glaucoma gene (GLC1A). *N Engl J Med*. 1998;338:1022–1027.
6. Gong G, Kosoko-Lasaki O, Haynatzki GR, Wilson MR. Genetic dissection of myocilin glaucoma. *Hum Mol Genet*. 2004;13 Spec No 1:R91–R102.
7. Shimizu S, Lichter PR, Johnson AT, et al. Age-dependent prevalence of mutations at the GLC1A locus in primary open-angle glaucoma. *Am J Ophthalmol*. 2000;130:165–177.
8. Ortego J, Escribano J, Coca-Prados M. Cloning and characterization of subtracted cDNAs from a human ciliary body library encoding TIGR, a protein involved in juvenile open angle glaucoma with homology to myosin and olfactomedin. *FEBS Lett*. 1997;413:349–353.
9. Torrado M, Trivedi R, Zinovieva R, Karavanova I, Tomarev SI. Optimedin: a novel olfactomedin-related protein that interacts with myocilin. *Hum Mol Genet*. 2002;11:1291–1301.
10. Ohlmann A, Goldwich A, Flugel-Koch C, Fuchs AV, Schwager K, Tamm ER. Secreted glycoprotein myocilin is a component of the myelin sheath in peripheral nerves. *Glia*. 2003;43:128–140.
11. Kim BS, Savinova OV, Reedy MV, et al. Targeted disruption of the myocilin gene (*Myoc*) suggests that human glaucoma-causing mutations are gain of function. *Mol Cell Biol*. 2001; 21:7707–7713.
12. Gould DB, Miceli-Libby L, Savinova OV, et al. Genetically increasing Myoc expression supports a necessary pathologic role of abnormal proteins in glaucoma. *Mol Cell Biol*. 2004; 24:9019–9025.
13. Senatorov V, Malyukova I, Fariss R, et al. Expression of mutated mouse myocilin induces open-angle glaucoma in transgenic mice. *J Neurosci*. 2006;26:11903–11914.
14. Zhou Y, Grinchuk O, Tomarev SI. Transgenic mice expressing the Tyr437His mutant of human myocilin protein develop glaucoma. *Invest Ophthalmol Vis Sci*. 2008;49:1932–1939.
15. Gould DB, Reedy M, Wilson LA, Smith RS, Johnson RL, John SW. Mutant myocilin nonsecretion in vivo is not sufficient to cause glaucoma. *Mol Cell Biol*. 2006;26:8427–8436.
16. Zode GS, Kuehn MH, Nishimura DY, et al. Reduction of ER stress via a chemical chaperone prevents disease phenotypes in a mouse model of primary open angle glaucoma. *J Clin Invest*. 2011;121:3542–3553.
17. Kwon HS, Johnson TV, Joe MK, et al. Myocilin mediates myelination in the peripheral nervous system through ErbB2/3 signaling. *J Biol Chem*. 2013;288:26357–26371.
18. Kwon HS, Nakaya N, Abu-Asab M, Kim HS, Tomarev SI. Myocilin is involved in Ngr1/Lingo-1-mediated oligodendrocyte differentiation and myelination of the optic nerve. *J Neurosci*. 2014;34:5539–5551.
19. Joe MK, Kee C, Tomarev SI. Myocilin interacts with syntrophins and is member of dystrophin-associated protein complex. *J Biol Chem*. 2012;287:13216–13227.
20. Jacobson N, Andrews M, Shepard AR, et al. Non-secretion of mutant proteins of the glaucoma gene myocilin in cultured trabecular meshwork cells and in aqueous humor. *Hum Mol Genet*. 2001;10:117–125.
21. Malyukova I, Lee HS, Fariss RN, Tomarev SI. Mutated mouse and human myocilins have similar properties and do not block general secretory pathway. *Invest Ophthalmol Vis Sci*. 2006;47:206–212.
22. Joe MK, Sohn S, Hur W, Moon Y, Choi YR, Kee C. Accumulation of mutant myocilins in ER leads to ER stress and potential cytotoxicity in human trabecular meshwork cells. *Biochem Biophys Res Comm*. 2003;312:592–600.
23. Joe MK, Tomarev SI. Expression of myocilin mutants sensitizes cells to oxidative stress-induced apoptosis. Implication for glaucoma pathogenesis. *Am J Pathol*. 2010;176: 2880–2890.
24. Sohn S, Hur W, Joe MK, et al. Expression of wild-type and truncated myocilins in trabecular meshwork cells: their

subcellular localizations and cytotoxicities. *Invest Ophthalmol Vis Sci*. 2002;43:3680–3685.

25. Stothert AR, Fontaine SN, Sabbagh JJ, Dickey CA. Targeting the ER-autophagy system in the trabecular meshwork to treat glaucoma. *Exp Eye Res*. 2016;144:38–45.
26. Anholt RR, Carbone MA. A molecular mechanism for glaucoma: endoplasmic reticulum stress and the unfolded protein response. *Trends Mol Med*. 2013;19:586–593.
27. Joe MK, Nakaya N, Abu-Asab M, Tomarev SI. Mutated myocilin and heterozygous Sod2 deficiency act synergistically in a mouse model of open-angle glaucoma. *Hum Mol Genet*. 2015; 24:3322–3334.
28. Oti M, Snel B, Huynen MA, Brunner HG. Predicting disease genes using protein-protein interactions. *J Med Genet*. 2006; 43:691–698.
29. Barabasi AL, Gulbahce N, Loscalzo J. Network medicine: a network-based approach to human disease. *Nat Rev Genet*. 2011;12:56–68.
30. Ideker T, Sharan R. Protein networks in disease. *Genome Res*. 2008;18:644–652.
31. Weber BH, Vogt G, Pruett RC, Stohr H, Felbor U. Mutations in the tissue inhibitor of metalloproteinases-3 (TIMP3) in patients with sorsby's fundus dystrophy. *Nat Genet*. 1994;8: 352–356.
32. Chen W, Stambolian D, Edwards AO, et al. Genetic variants near TIMP3 and high-density lipoprotein-associated loci influence susceptibility to age-related macular degeneration. *Proc Natl Acad Sci U S A*. 2010;107:7401–7406.
33. Fritsche LG, Igl W, Bailey JN, et al. A large genome-wide association study of age-related macular degeneration highlights contributions of rare and common variants. *Nat Genet*. 2016;48:134–143.
34. Kwon HS, Lee HS, Ji Y, Rubin JS, Tomarev SI. Myocilin is a modulator of Wnt signaling. *Mol Cell Biol*. 2009;29:2139–2154.
35. Nakaya N, Sultana A, Munasinghe J, Cheng A, Mattson MP, Tomarev SI. Deletion in the N-terminal half of olfactomedin 1 modifies its interaction with synaptic proteins and causes brain dystrophy and abnormal behavior in mice. *Exp Neurol*. 2013;250:205–218.
36. Craig R, Cortens JC, Fenyo D, Beavis RC. Using annotated peptide mass spectrum libraries for protein identification. *J Proteome Res*. 2006;5:1843–1849.
37. Bjornson RD, Carriero NJ, Colangelo C, et al. X!!Tandem, an improved method for running x!Tandem in parallel on collections of commodity computers. *J Proteome Res*. 2008; 7:293–299.
38. Comeau SR, Gatchell DW, Vajda S, Camacho CJ. ClusPro: a fully automated algorithm for protein-protein docking. *Nucleic Acids Res*. 2004;32:W96–W99.
39. Emsley P, Lohkamp B, Scott WG, Cowtan K. Features and development of Coot. *Acta Crystallogr D Biol Crystallogr*. 2010;66:486–501.
40. Takahashi H, Noda S, Imamura Y, et al. Mouse myocilin (Myoc) gene expression in ocular tissues. *Biochem Biophys Res Commun*. 1998;248:104–109.
41. Swiderski RE, Ross JL, Fingert JH, et al. Localization of *MYOC* transcripts in human eye and optic nerve by in situ hybridization. *Invest Ophthalmol Vis Sci*. 2000;41:3420–3428.
42. Donegan RK, Hill SE, Freeman DM, et al. Structural basis for misfolding in myocilin-associated glaucoma. *Hum Mol Genet*. 2015;24:2111–2124.
43. Wisniewska M, Goettig P, Maskos K, et al. Structural determinants of the adam inhibition by TIMP-3: crystal structure of the TACE-N-TIMP-3 complex. *J Mol Biol*. 2008; 381:1307–1319.
44. Chong NH, Alexander RA, Gin T, Bird AC, Luthert PJ. TIMP-3, collagen, and elastin immunohistochemistry and histopathology of Sorsby's fundus dystrophy. *Invest Ophthalmol Vis Sci*. 2000;41:898–902.
45. Fariss RN, Apte SS, Olsen BR, Iwata K, Milam AH. Tissue inhibitor of metalloproteinases-3 is a component of bruch's membrane of the eye. *Am J Pathol*. 1997;150:323–328.
46. Carnevale D, Pallante F, Fardella V, et al. The angiogenic factor plgf mediates a neuroimmune interaction in the spleen to allow the onset of hypertension. *Immunity*. 2014;41:737–752.
47. Oh DJ, Martin JL, Williams AJ, Russell P, Birk DE, Rhee DJ. Effect of latanoprost on the expression of matrix metalloproteinases and their tissue inhibitors in human trabecular meshwork cells. *Invest Ophthalmol Vis Sci*. 2006;47:3887–3895.
48. Ashworth Briggs EL, Toh T, Eri R, Hewitt AW, Cook AL. TIMP1, TIMP2, and TIMP4 are increased in aqueous humor from primary open angle glaucoma patients. *Mol Vis*. 2015;21: 1162–1172.
49. Hussain AA, Lee Y, Zhang JJ, Marshall J. Disturbed matrix metalloproteinase activity of Bruch's membrane in age-related macular degeneration. *Invest Ophthalmol Vis Sci*. 2011;52: 4459–4466.
50. Jia Y, Hu DN, Zhu D, et al. MMP-2, MMP-3, TIMP-1, TIMP-2, and TIMP-3 protein levels in human aqueous humor: relationship with axial length. *Invest Ophthalmol Vis Sci*. 2014;55:3922–3928.
51. Ronkko S, Rekonen P, Kaarniranta K, Puustjarvi T, Terasvirta M, Uusitalo H. Matrix metalloproteinases and their inhibitors in the chamber angle of normal eyes and patients with primary open-angle glaucoma and exfoliation glaucoma. *Graefes Arch Clin Exp Ophthalmol*. 2007;245:697–704.
52. Brew K, Dinakarpandian D, Nagase H. Tissue inhibitors of metalloproteinases: evolution, structure and function. *Biochim Biophys Acta*. 2000;1477:267–283.
53. Kessenbrock K, Wang CY, Werb Z. Matrix metalloproteinases in stem cell regulation and cancer. *Matrix Biol*. 2015;44–46: 184–190.
54. Page-McCaw A, Ewald AJ, Werb Z. Matrix metalloproteinases and the regulation of tissue remodelling. *Nat Rev Mol Cell Biol*. 2007;8:221–233.
55. Joe MK, Kwon HS, Cojocaru R, Tomarev SI. Myocilin regulates cell proliferation and survival. *J Biol Chem*. 2014;289:10155–10167.
56. De Groef L, Van Hove I, Dekeyster E, Stalmans I, Moons L. MMPs in the neuroretina and optic nerve: modulators of glaucoma pathogenesis and repair? *Invest Ophthalmol Vis Sci*. 2014;55:1953–1964.
57. Sivak JM, Fini ME. MMPs in the eye: emerging roles for matrix metalloproteinases in ocular physiology. *Prog Retin Eye Res*. 2002;21:1–14.
58. Bradley JM, Kelley MJ, Zhu X, Anderssohn AM, Alexander JP, Acott TS. Effects of mechanical stretching on trabecular matrix metalloproteinases. *Invest Ophthalmol Vis Sci*. 2001; 42:1505–1513.
59. Husain S, Jafri F, Crosson CE. Acute effects of PGF2alpha on MMP-2 secretion from human ciliary muscle cells: a PKC- and ERK-dependent process. *Invest Ophthalmol Vis Sci*. 2005;46: 1706–1713.
60. Kumar S, Shah S, Tang HM, Smith M, Borras T, Danias J. Tissue plasminogen activator in trabecular meshwork attenuates steroid induced outflow resistance in mice. *PLoS One*. 2013; 8:e72447.
61. Micera A, Quaranta L, Esposito G, et al. Differential protein expression profiles in glaucomatous trabecular meshwork: an evaluation study on a small primary open angle glaucoma population. *Adv Ther*. 2016;33:252–267.

Investigative Ophthalmology & Visual Science

62. Nga AD, Yap SL, Samsudin A, Abdul-Rahman PS, Hashim OH, Mimiwati Z. Matrix metalloproteinases and tissue inhibitors of metalloproteinases in the aqueous humour of patients with primary angle closure glaucoma - a quantitative study. *BMC Ophthalmol*. 2014;14:33.
63. Sohn EH, Khanna A, Tucker BA, Abramoff MD, Stone EM, Mullins RF. Structural and biochemical analyses of choroidal thickness in human donor eyes. *Invest Ophthalmol Vis Sci*. 2014;55:1352–1360.
64. Nishida Y, Fujiwara T, Imamura Y, Lima LH, Kurosaka D, Spaide RF. Choroidal thickness and visual acuity in highly myopic eyes. *Retina*. 2012;32:1229–1236.
65. Switzer DW Jr, Mendonca LS, Saito M, Zweifel SA, Spaide RF. Segregation of ophthalmoscopic characteristics according to choroidal thickness in patients with early age-related macular degeneration. *Retina*. 2012;32:1265–1271.
66. Ko A, Cao S, Pakzad-Vaezi K, Brasher PM, et al. Optical coherence tomography-based correlation between choroidal thickness and drusen load in dry age-related macular degeneration. *Retina*. 2013;33:1005–1010.
67. Pavloff N, Staskus PW, Kishnani NS, Hawkes SP. A new inhibitor of metalloproteinases from chicken: ChiMP-3. A third member of the TIMP family. *J Biol Chem*. 1992;267:17321–17326.
68. Lan J, Kumar RK, Di Girolamo N, McCluskey P, Wakefield D. Expression and distribution of matrix metalloproteinases and their inhibitors in the human iris and ciliary body. *Br J Ophthalmol*. 2003;87:208–211.
69. Vranka JA, Johnson E, Zhu X, et al. Discrete expression and distribution pattern of TIMP-3 in the human retina and choroid. *Curr Eye Res*. 1997;16:102–110.
70. Kamei M, Hollyfield JG. TIMP-3 in Bruch's membrane: changes during aging and in age-related macular degeneration. *Invest Ophthalmol Vis Sci*. 1999;40:2367–2375.
71. Della NG, Campochiaro PA, Zack DJ. Localization of TIMP-3 mRNA expression to the retinal pigment epithelium. *Invest Ophthalmol Vis Sci*. 1996;37:1921–1924.
72. Macosko EZ, Basu A, Satija R, et al. Highly parallel genome-wide expression profiling of individual cells using nanoliter droplets. *Cell*. 2015;161:1202–1214.
73. Fariss RN, Apte SS, Luthert PJ, Bird AC, Milam AH. Accumulation of tissue inhibitor of metalloproteinases-3 in human eyes with Sorsby's fundus dystrophy or retinitis pigmentosa. *Br J Ophthalmol*. 1998;82:1329–1334.

Investigative Ophthalmology & Visual Science